

New Techniques for Disconnecter Switching VFT Mitigation in GIS

MA Abd-Allah¹, A Said¹, Ebrahim A Badran²

¹Faculty of Engineering at Shoubra, Benha University, Egypt

²Faculty of Engineering, Mansoura University, Egypt

Article Info

Article history:

Received Nov 22, 2013

Revised Jan 16, 2014

Accepted Feb 7, 2014

Keyword:

GIS

VFT

Mitigation Techniques

EMTP/ATP

ABSTRACT

Switching operations in a Gas Insulated Substations (GIS) generate very fast transient over voltages (VFTO) which are dangerous for the transformer and the system insulation because of their short rise time. Under special circumstances the overvoltages can arise close to the transformer Basic Insulation Level (BIL). The reduction of VFTO amplitudes is considered main challenges. Therefore, VFTO in the 220 kV Wadi-Hoff GIS is analyzed and the worst case for disconnector switching is predicted using EMTP/ATP in this paper. VFTO mitigation techniques are studied in this work. Furthermore, proposed techniques are presented for mitigating the VFTO. The proposed techniques can be used by the maintenance engineers, transformer designers, and GIS insulation manufactures. The results show that the proposed techniques highly reduce the VFTO in a simple manner

Copyright © 2014 Institute of Advanced Engineering and Science.
All rights reserved.

Corresponding Author:

A Said,

Faculty of Engineering at Shoubra, Benha University, Egypt

Email: abdelrahman.ghoniem@feng.bu.edu.eg

1. INTRODUCTION

GIS is widely used in electric power system in recent decades because of its advantages such as compact size, protection from pollution, a few maintenance, and high reliability. In spite of these advantages, GIS has unique problems, such as the very fast voltage increase due to reflections of switching transients at various junctions within the GIS [1-2]. These transients are originated within the GIS any time there is an instantaneous change in voltage. They have very short rise times, in the range of 4 to 100 ns, and are normally followed by oscillations having frequencies in the range of 100 kHz to 50 MHz [2]. They cause traveling waves internally inside the GIS, traveling from GIS bushing to external components. This can lead to damage the insulation of internal busbar and transformer, which influent the operating reliability of GIS, accelerate aging of transformer insulation and reduce transformer life [1-3]. Also, VFTO associated with Very Fast Transient Currents (VFTC) radiate electromagnetic fields during its propagation through the coaxial GIS bus section. The transient electromagnetic fields get coupled to the control equipment or data cables of the GIS [4].

In fact, the response behavior of zinc oxide (ZnO) surge arresters to such Very Fast Transients (VFT) is not well characterized, and the turn-on time of ZnO surge arresters may be much longer than the rise times of the VFT. Therefore, the traditional ZnO surge arresters cannot suppress the wave steepness because surge arresters do not act fast enough to prevent the switching transients with steep front [5].

This paper investigates the VFTO resulted from the operation of disconnector switches at different sensitive points internal and external the 220 kV Wadi-Hoff GIS. The 220 kV Wadi-Hoff GIS is taken as a case study. Therefore, VFTO in the 220 kV Wadi-Hoff GIS is analyzed and the worst case for disconnector switching is predicted using EMTP/ATP.

VFTO mitigation techniques are studied in this work. Furthermore, in this paper, proposed techniques are presented for mitigating the VFTO. The proposed techniques can be used by the maintenance

engineers, transformer designers, and GIS insulation manufactures. The results show that the proposed techniques highly reduce the VFTO in a simple manner.

2. MODELING OF THE 220 KV WADI-HOFF GIS

Due to the traveling nature of the transients, the different components can be modeled by distributed parameter lines, surge impedances and traveling times. Each GIS section is simulated by its equivalent capacitance and inductance, which can be determined as follows [6-7].

$$C = \frac{2\pi\epsilon}{\ln D/d} \quad (\epsilon \approx \epsilon_0) \quad F / m \quad (1)$$

$$L = \frac{\mu \ln \frac{D}{d}}{2\pi} \quad H / m \quad (2)$$

$$Z_0 = \sqrt{L/C} = \frac{\sqrt{\epsilon\mu}}{2\pi} \ln \frac{D}{d} \approx 60 \ln \frac{D}{d} \quad \Omega \quad (3)$$

$$v = \frac{1}{\sqrt{LC}} \quad m / s \quad (4)$$

where C and L are the capacitance and the inductance of the GIS busbar, respectively. d is the outside diameter of the GIS busbar and D is the inner diameter of the GIS enclosure. Z₀ is the surge impedance and v is the propagation velocity.

The single line diagram of the substation under study is illustrated in Figure 1. The 220/66/11 kV Wadi-Hoff substation under study consists of four incoming feeders, two feeders each of 30 km length, and the other two feeders each of 3 km length. The substation includes three 125 MVA, 220/66/11 kV, power transformers. The feeders are connected in a two busbar arrangement with a bus coupler. The equivalent circuits of the different GIS components and the values of the different parameters in the simulation are summarized in Table 1.

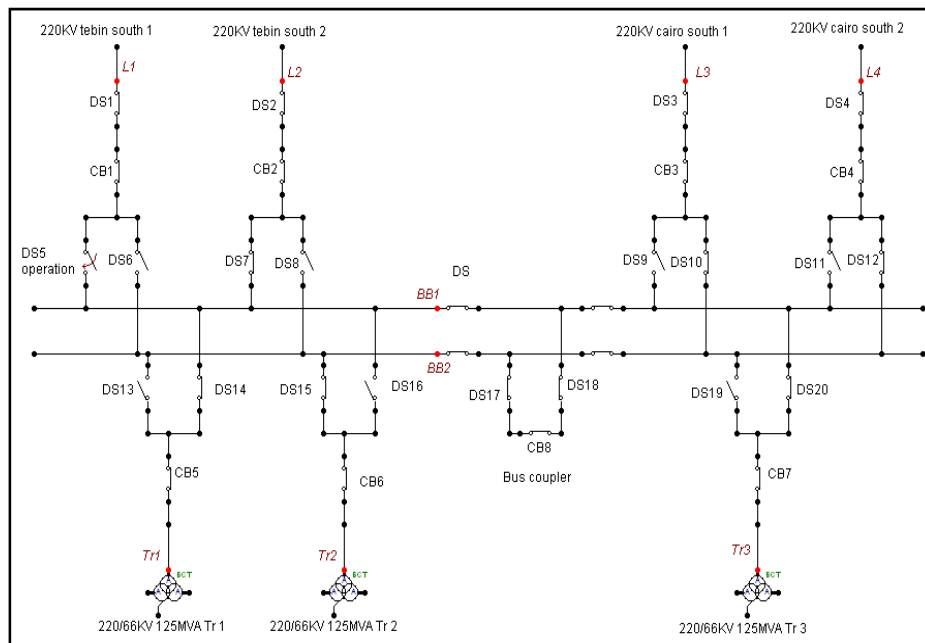


Figure 1. Typical single line diagram for Wadi-Hoff GIS

Table 1. Information for simulation

GIS Busbar	$Z_0 = 70 \Omega$ and $v=270 \text{ m}/\mu\text{s}$
Circuit Breaker	In the closed position: impedance of 70Ω In the open position: capacitances of 90 pF (either end to ground) and 50 pF (between contacts)
Disconnecter, and Earthing Switch	In the closed position: impedance of 70Ω In the open position: capacitances of 30 pF (either end to ground) and 30 pF (between contacts)
Potential Transformer	Capacitance of 100 pF towards ground
Current transformer	$Z_0 = 70 \Omega$ and $v=270 \text{ m}/\mu\text{s}$
Surge Arrester	200 pF in series with a grounding resistance of 0.1Ω .
Overhead Transmission Line	$Z_0 = 250 \Omega$ and $v=300 \text{ m}/\mu\text{s}$
Elbows, Spacers, and Spherical Shields	lumped capacitance of 15 pF towards ground
Bushing	Impedance of 70Ω and 100 pF towards ground

The behavior of the spark in disconnector operations can be represented by a dynamically variable resistance with a controllable collapse time [1]. The disconnector switch (DS) restrikes are modeled as an exponentially decaying resistance in series with a small resistance. This is implemented using a Type-91, TACS time-varied resistance in EMTP/ ATP. The variable resistance is calculated from the following equation:

$$R(t) = R(0)e^{-\frac{t}{\tau}} + r \quad (5)$$

where $R(0)$ is 10^{12} ohm and the time constant t is 1 ns . r represents the spark resistance after voltage breakdown and is assumed to be 0.5Ω [2, 3, 8]. During the GIS DS closing operation, the voltage breakdown takes about 4 ns , so the DS closing event is modeled as an exponentially decreasing resistance. The nonlinear resistance decreases from high value (10^{12}) to 0.5Ω in about 5 ns as shown in Figure 2.

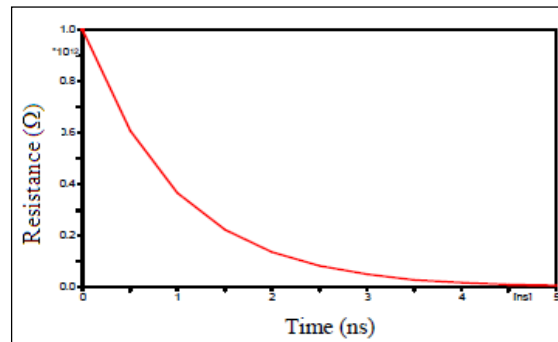


Figure 2. DS resistance behavior during closing event

At high frequencies, the winding of transformer behaves like a capacitive network consisting of series capacitances between turns and coils, and shunt capacitances between turns and coils to the grounded core and transformer tank. So, the transformers are simulated in this work by their surge capacitances. These equivalent capacitances are in the range from 2 to 10 nF [1, 2, 3]. The transformer is modeled as a capacitor with 2 nF as given in [2]. EMTP/ATP is used to simulate the substation under study. Figure 3 illustrates the 220 kV Wadi-Hoff GIS model in EMTP/ATP.

3. OVERVOLTAGES OF DISCONNECTOR SWITCHING

There are several switching operations to achieve some purpose such as energizing feeders, energizing transformer, CB maintenance, etc. At energizing feeders or transformer, disconnector is closed firstly, and then the CB is closed.

Table 2 shows different operating modes of disconnectors in the studied system.

At the operating modes of disconnector, the VFTO is calculated at the internal points of GIS (BB1 and BB2), the transformers terminals (Tr1, Tr2, and Tr3) and the GIS terminals such as at SF6/air bushing (L1, L2, L3, and L4). Figure 4 shows the VFTO at several points due to different operating modes of disconnector switching. It can be seen that mode#1 is the worst case of disconnector operation in the studied substation. It is observed that the peak magnitude of the generated VFTO at Tr1 is about 2.04 pu, while it is about 1.60 pu at Tr2, 1.58 pu at Tr3, 1.44 pu at L2, 1.14 pu at L3, 1.13 pu at L4, 1.22 pu at BB1 and 1.14 pu at BB2. Also, the wave shape of the generated VFTO at Tr1 is shown in Figure 5.

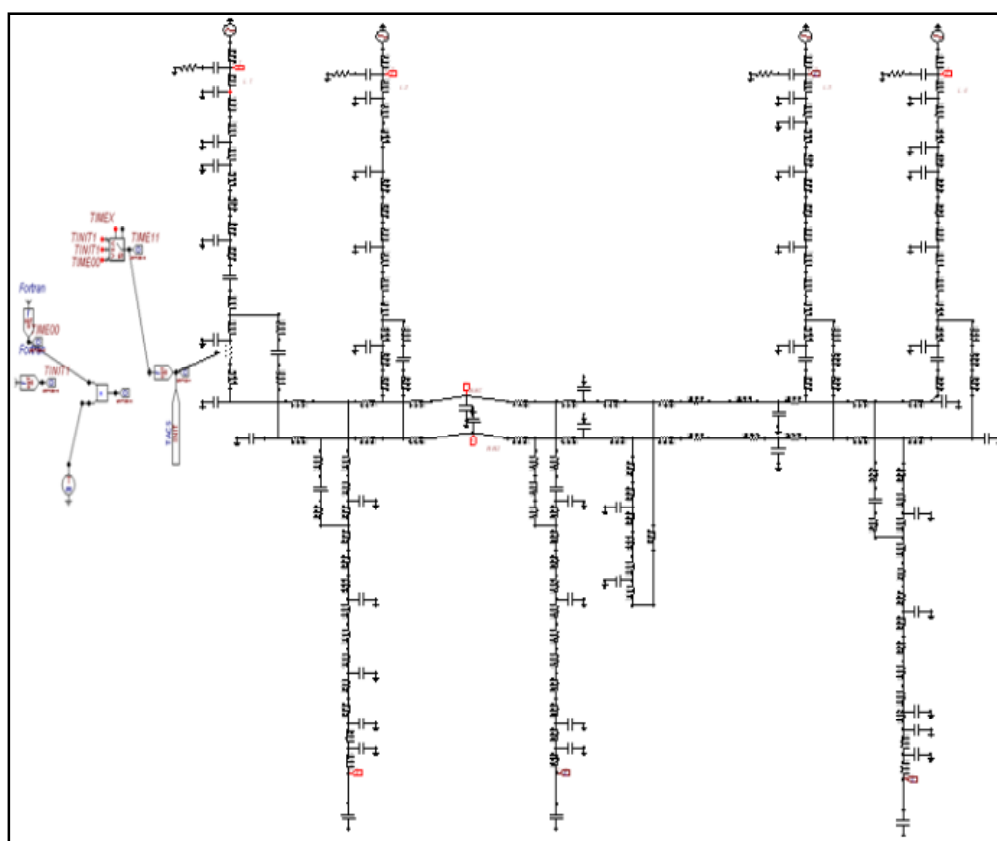


Figure 3. EMTP/ATP Model for Wadi-Hoff GIS

Table 2. Operating modes of various disconnectors in 220 kV

Mode	Power Supply	Opened CB	Operating DS
#1	line 1 out	CB1	DS 5
#2	line 2 out	CB2	DS 7
#3	line 3 out	CB3	DS 10
#4	line 4 out	CB4	DS 12
#5	All lines connected	CB5	DS 14
#6	All lines connected	CB6	DS 15
#7	All lines connected	CB7	DS 20

4. VFTO SUPPRESSION TECHNIQUES

Up to date, the main challenges are the reduction of VFTO amplitudes. The researchers concerns on finding the optimum technique for suppressing VFTO. Several techniques are used to reduce the harmful effects of the VFTO [2, 5, 7, 8, 9]. The important techniques are studied in this work to choice the suitable technique for suppressing the VFTO value to a safe one [9].

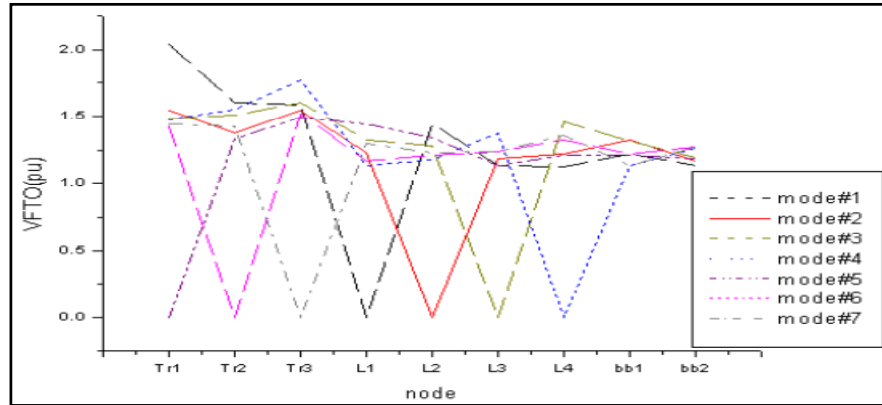


Figure 4. Comparison between Several Modes of Disconnecter Operation

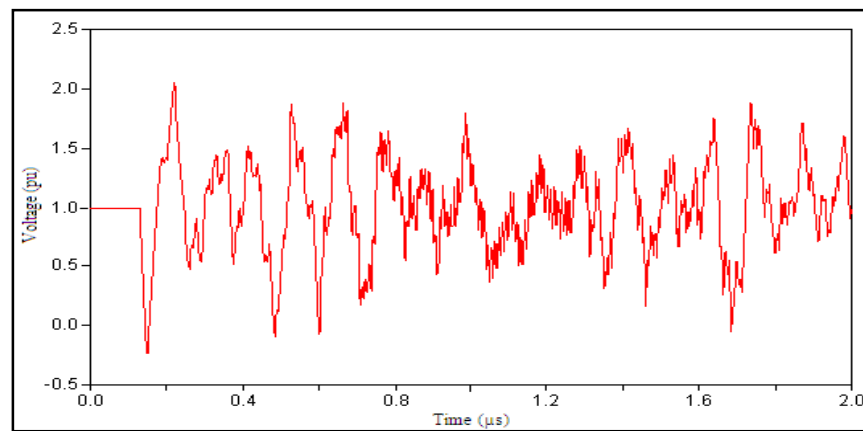


Figure 5. VFTO at Tr1 (Worst Case)

4.1. The Appropriate Load Side Terminals

The peak magnitude and frequency content of VFT depends on the terminal component connected to the GIS. The terminal components can be cables, gas-insulated lines (GIL), or overhead transmission lines (OHTL). Table 3 gives the electric parameters of these terminal components.

Table 3. Terminal component data

Terminal component	Surge impedance (Ω)	Propagation velocity, v_p (m/ μ s)
GIL	70	270
OHTL	250	300
XLPE Cable	30	165

The attenuation of VFT with time depends on the type and length of load side terminal component connected to the GIS [8]. Therefore, the VFT can be mitigated by replacement with the appropriate terminals. Simplicity, low cost implementation, and minimum changes in the installed GIS are the main advantages of this technique. Practically in Wadi-Hoff GIS, 5 m OHTL on the source side terminals and 11 m OHTL on the load side terminals are used. It is clear that the lowest values occur with using cable terminations. Also, the peak values decreased with increasing the cable length. These can be explained as; the cable attenuates the VFTO due to its capacitance to ground, which effectively reduced the VFTO magnitude. Figure 6 shows the effect of terminal length on VFTO peak at Tr1. It is clearly seen that with length increases the VFTO reduces. Also, Figure 7 illustrates a comparison between the VFTO at Tr1 in two load terminal cases; 11 m OHTL and 11 m cable.

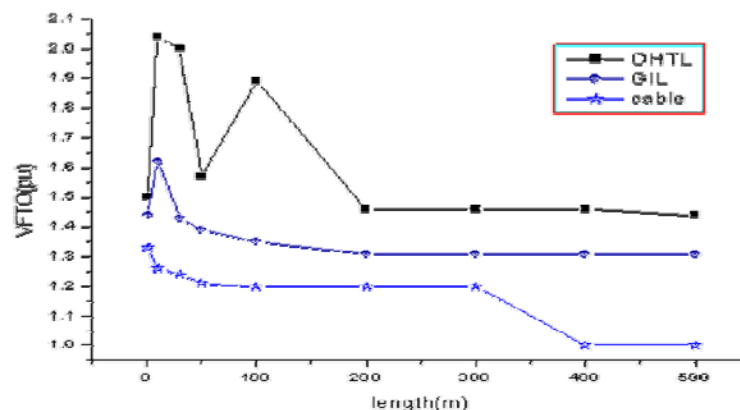


Figure 6. The peak of the VFTO at Tr1 terminal Vs the load-side terminal length

4.2. The Capacitance at Transformer Terminal

Lumped shunt capacitance is used to damp the VFTO in many applications. The capacitance is arising in surge arrestors, capacitive voltage transformers (CVT), cables, or additional capacitor on the transformer terminals. The capacitance value is changed according to the specifications of the system. Many researches use the capacitance with different values [2, 10]. Table 5 gives the effect of the shunt capacitance at the transformer terminals. It is clearly seen that, by increasing the capacitance, the VFTO due to DS re-striking will be further reduced at transformers terminals (Tr1, Tr2, and Tr3). This effect is greatly shown for capacitance values from 0.1 nF to 10 nF, whereas the values above 10 nF do not affect on the results.

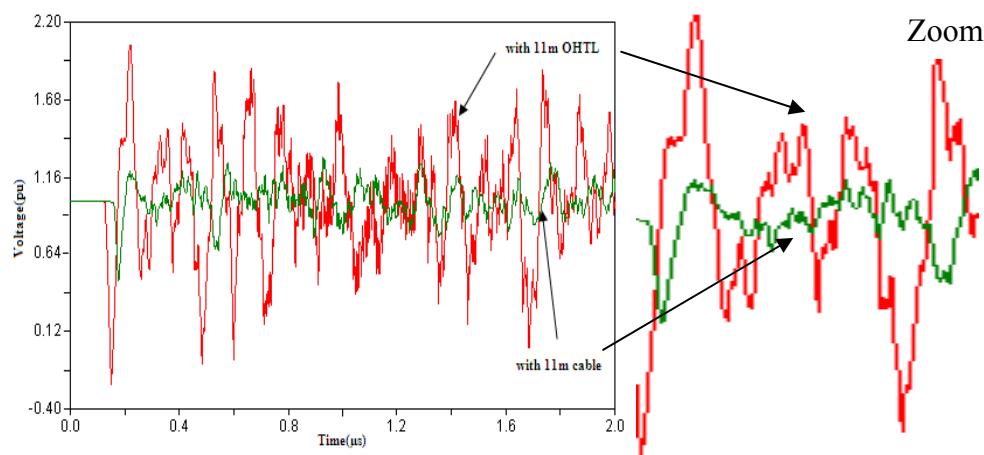


Figure 7. Comparison between the VFTO at Tr1 in case of OHTL and Cable load terminals

Table 4. Effect of lumped capacitance on VFTO and VFTC

Capacitance (nF)	Tr1		Tr2		Tr3	
	VFTO (pu)	VFTC (pu)	VFTO (pu)	VFTC (pu)	VFTO (pu)	VFTC (pu)
Without	2.04	0.87e-15	1.60	0.21e-31	1.58	0.61e-15
0.1	1.49	0.14e-14	1.21	0.12e-14	1.30	0.13e-14
0.8	1.11	0.30e-14	1.06	0.89e-14	1.06	0.89e-14
1.0	1.08	0.90e-14	1.06	0.91e-14	1.06	0.90e-14
10	1.01	0.72e-13	1	0.67e-13	1.06	0.67e-13
50	1	0.89e-13	1	0.10e-12	1	0.95e-13
100	1	0.62e-12	1	0.62e-12	1	0.62e-12

Figure 8 shows the influence of the capacitance component on the VFTO and the VFTC at Tr1. Figure 8 can be used to provide a solution for choosing the optimum value of the capacitance components. This optimum point is achieved at the intersection point of the two curves. So, the adding an extra surge arrester which has a capacitance around 10 nF (the optimum value) can help to achieve the optimum point at Tr1, Tr2, and Tr3.

In order to reduce the VFT at the power transformer, the application of surge capacitors is a feasible alternative due to space limitation and cost, if the suitable capacitance value is selected. Because of impossibility of adding capacitance in high voltage systems, the coupling capacitor voltage transformer with capacitance of 10nF is utilized instead of potential transformer [2].

Figure 9 illustrates a comparison between the VFTO at Tr1 in case of without and with a capacitance of 10 nF. It is clearly seen the high reduction of oscillations and the value of VFTO.

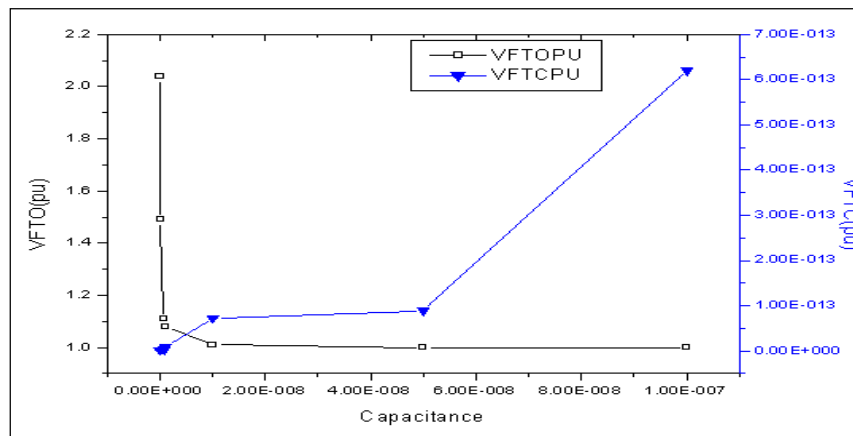


Figure 8. Influence of Capacitance Component on VFTO and VFTC at Tr1

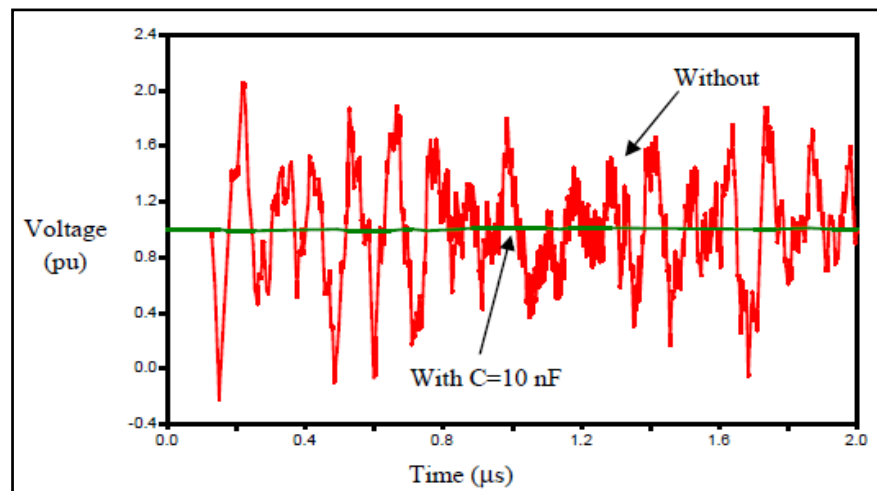


Figure 9. Comparison between the VFTO at Tr1 in case of without and with shunt capacitance

4.3. Shunt Resistor Disconnect Switching

The switching resistance is connected in parallel with the contacts of the disconnect switch. With the arc to be shunted by the resistance, a part of the arc current flows through the resistance, the arc current will decrease and the rate of deionization of the arc path will be increased [9, 10].

The installation of opening and closing resistor has a certain application in order to inhibit the generated VFTO in GIS [9]. The shunt resistor acts as a buffering element to the transient process, leaking the remaining charge and absorbing the overvoltage energy. Shunt resistance accelerates the decay of the transient process.

Figure 10 shows the VFTO when the shunt resistor is used. The effect of changing the resistance value on the VFTO at several points in GIS is used. The amplitude of VFTO is decreased as the switching resistance increases. With increasing the switching resistance from 0 to 400 ohm, the VFTO noticeably decreases. As the switching resistance increased beyond 400 ohm, the VFTO decreased slowly.

It is shown that at the switching resistance of 400 Ω , an optimum solution is get. Furthermore, the maximum voltage to ground at each component and the percentage of voltage increasing are given in Table 6. Figure 11 shows the comparison between the voltage waveforms of Tr1 in case of with and without shunt resistance.

Table 6. Effect of Shunt Resistance on VFTO

Case	VFTO (pu)								
	Tr1	Tr2	Tr3	L1	L2	L3	L4	BB1	BB2
Without shunt resistor	2.04	1.60	1.58	0	1.44	1.14	1.13	1.22	1.14
With shunt resistor of 400 Ω	1.14	1.09	1.08	0	1.04	1.03	1.04	1.04	1.04
% Reduction	44	31	31	0	27	19	9	14	9

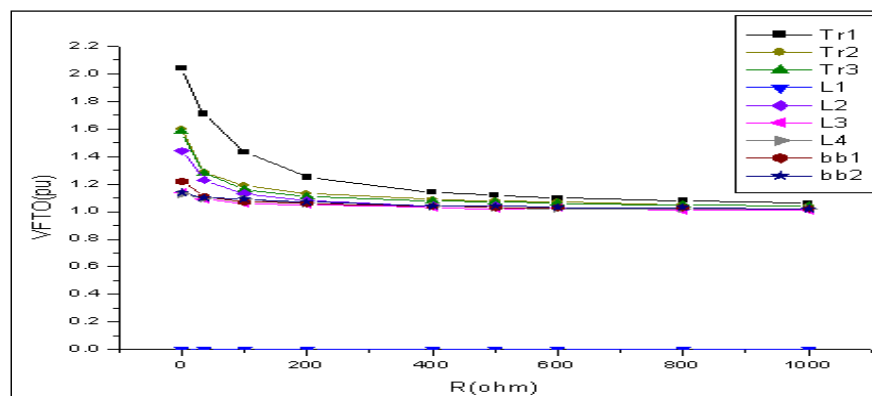


Figure 10. VFTO at GIS Terminals Vs switching resistor value

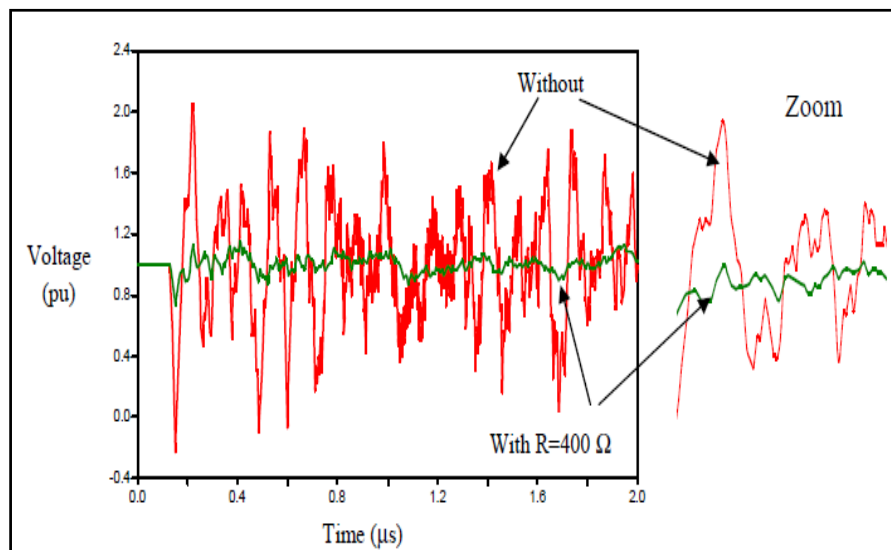


Figure 11. VFTO at Tr1 with and without shunt resistance

4.4. Ferrite Rings Technique

Ferrite is a high-frequency nonlinear magnetic material. The ferrite rings is used around GIS conductors to absorb the transient energy when the DS restrikes to inhibit the VFTO. The ferrite rings can be simplified to a nonlinear inductance and a nonlinear resistance, in series with GIS conductor [7, 8].

A ferrite rings of length of 0.47 m with an equivalent diameter of 0.15 m, having an equivalent resistor of $70\ \Omega$ and an equivalent inductance of 0.02 mH is used in this study.

Table 7 shows the variation of VFTO at several points due to using many ferrite rings. The results show that the increasing of the number of rings from 1 to 3 gives great effect on reducing the VFTO. More rings gives small effect on the VFTO. So, the optimum result is found with using 3 rings. Figure 12 illustrates the VFTO when 3 ferrite rings are used at Tr1. It is clearly seen from Table 7 that the reduction of the VFTO is 20% at Tr1, 7% at Tr2, 6% at Tr3, 7% at L2, 2% at L3 and L4, and 2% at BB1 and BB2.

Table 7. Variation of VFTO with the number of ferrite rings

No of rings	VFTO (pu)								
	Tr1	Tr2	Tr3	L1	L2	L3	L4	BB1	BB2
1	1.45	1.23	1.20	0	1.17	1.08	1.10	1.09	1.10
2	1.33	1.17	1.14	0	1.11	1.06	1.08	1.07	1.08
3	1.23	1.14	1.12	0	1.08	1.05	1.06	1.06	1.07
4	1.20	1.12	1.11	0	1.06	1.04	1.05	1.05	1.06
5	1.18	1.11	1.10	0	1.05	1.04	1.04	1.05	1.05
6	1.15	1.10	1.09	0	1.04	1.03	1.03	1.05	1.05

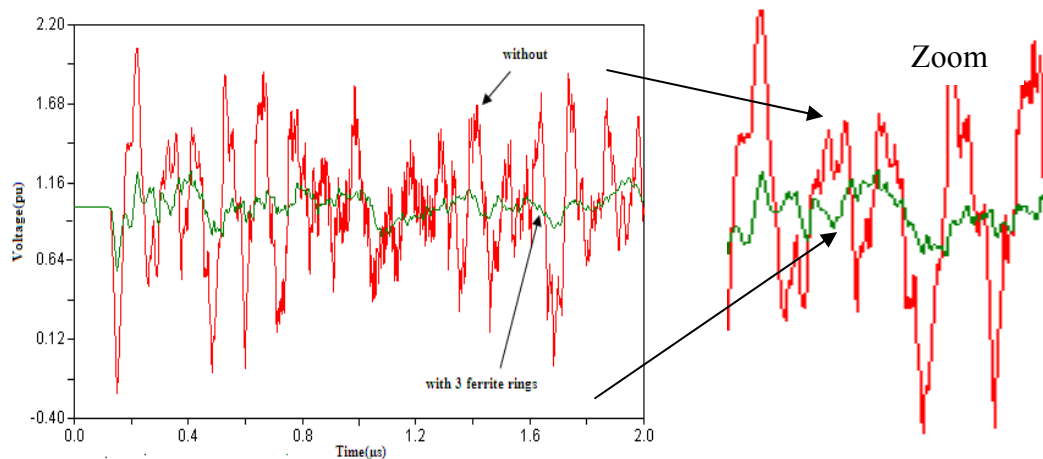


Figure 12. VFTO at Tr1 with and without ferrite rings

4.5. RC Filter

RC filters (R in parallel with C) have been widely used to protect loads. Also, they have been widely used in vacuum circuit breakers to suppress the over voltages of the arcing [7]. R is used to make energy attenuates and C reduces the circuit oscillation frequency. In this work RC filter is used as a shunt component next to the main transformer to protect it. R is varied from $50\ \Omega$ to $400\ \Omega$ and C is changed from 0.01 to 0.2 μF [7]. The optimum mitigation of the VFTO is found at R equal to $50\ \Omega$ and at C equal to 0.01 μF .

Table 8 shows the variation of VFTO at several points due to using the RC filter. Also, the percentage reduction in over voltages is given. It is clearly seen that this technique only protects the transformers, whereas the other points in GIS do not affected. Figure 13 illustrates the comparison between VFTO at Tr1 in case of with and without the RC filter.

Table 8. Variation of VFTO at several points due to using the RC filter

Case	VFTO (pu)								
	Tr1	Tr2	Tr3	L1	L2	L3	L4	BB1	BB2
Without shunt RC filter	2.04	1.60	1.58	0	1.44	1.14	1.13	1.22	1.14
With shunt RC filter	1.008	1.0071	1.006	0	1.44	1.14	1.13	1.22	1.14
% Reduction	50	37	36	0	0	0	0	0	0

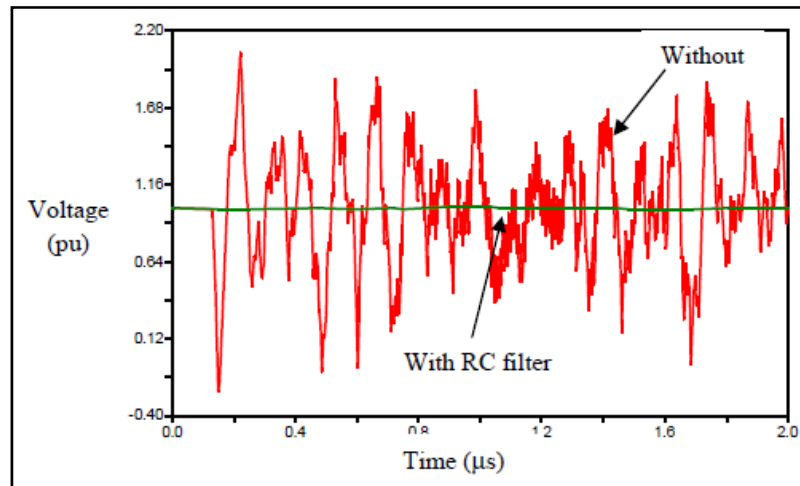


Figure 13. Comparison between VFTO at Tr1 with and without RC Filter

5. THE PROPOSED TECHNIQUES FOR VFT MITIGATION IN GIS

Increasing the shunt resistor value gives a reduction of VFTO but this is still associated with high oscillations, as given in section 4.3. Therefore, these oscillations can be fitted by a capacitor or an inductor in series with the resistor. In the following subsections the two techniques are investigated.

5.1. Shunted Series RC

When resistance fixed at 400Ω and change capacitance value if increase capacitances above $1\mu\text{F}$ find no change on VFTO peak and if reduces capacitance below $1\mu\text{F}$ find great change on reduction of VFTO peak.

Table 9 gives the VFTO at the GIS terminals in case of without and with shunted series RC. Also, the percentage reduction is given. It is found that the reduction is more than that when the shunted resistor is used (as given in Table 6). Figure 14 shows a comparison between the VFTO at Tr1 in case of with and without shunted series RC, where R is 400Ω and C is 1pF .

Furthermore, Figure 15 gives a comparison between the VFTO at Tr1 when a shunted resistor of 400Ω is used and the proposed shunted series RC with the same resistance and C is 1pF . The figure clearly illustrates the reduction in both the VFTO magnitude and oscillation in case of the proposed technique.

Table 9. VFTO at several points due to using the shunted series RC

Case	VFTO (pu)								
	Tr1	Tr2	Tr3	L1	L2	L3	L4	bb1	bb2
Without	2.04	1.60	1.58	0	1.44	1.14	1.13	1.22	1.14
With shunted Series RC, $R = 400\Omega + C = 1\text{pF}$	1.01	1.01	1.01	0	1.04	1.00	1.00	1.00	1.00
% Reduction	50	37	36	0	30	20	11	18	12

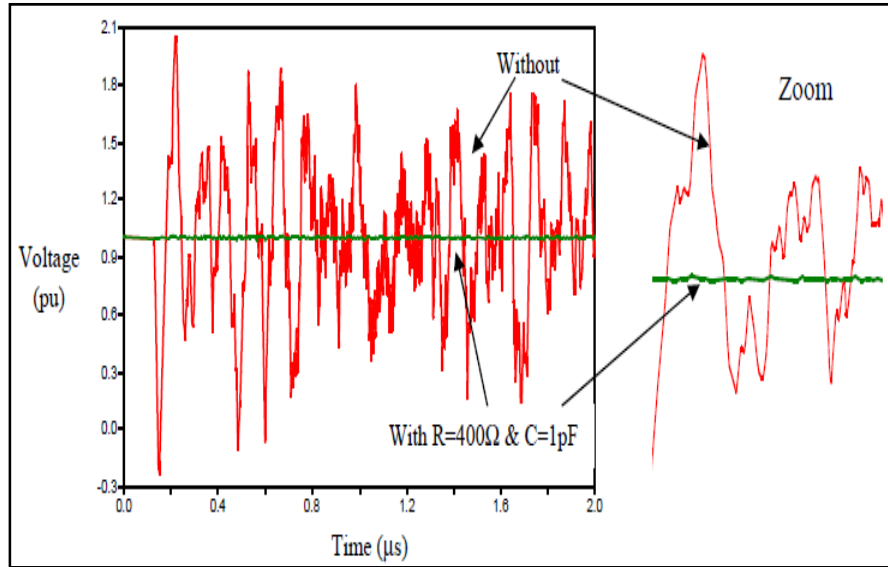


Figure 14. VFTO at Tr1 with and without shunted series RC

5.2. Shunted Series RL Disconnecter Switch

The using of an inductor can limit the dv/dt at transformer terminals. So, shunted series RL is proposed to mitigate the VFTO. The series resistance is chosen as 400Ω as given in section 4.3 and the series inductance is changed to select the suitable value for this study.

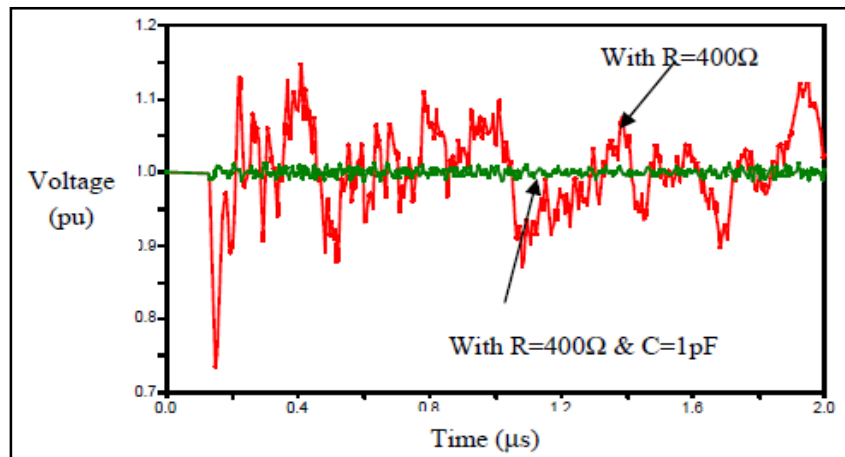


Figure 15. Comparison between the VFTO when either the shunt resistance or the proposed shunted series RC

Table 10 shows the VFTO when several values of the inductance are applied in series with a 400Ω resistance. It is found that the VFTO decreases with the inductance increasing. Figure 16 illustrates a comparison between VFTO in case of without and with the proposed shunted series RL.

Table 10. VFTO due to the proposed shunted series RL, ($R=400 \Omega$)

Inductance in mH	VFTO (pu)								
	Tr1	Tr2	Tr3	L1	L2	L3	L4	bb1	bb2
0.01	1.11	1.08	1.08	0	1.04	1.03	1.03	1.02	1.03
0.1	1.05	1.04	1.04	0	1.01	1.01	1.01	1.03	1.03
1	1	1	1	0	1	1	1	1	1

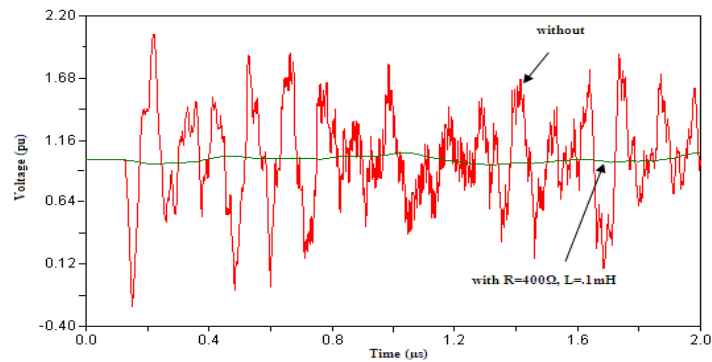


Figure 16. VFTO at Tr1 with and without shunted series RL

Also, Figure 17 illustrates a comparison between the VFTO at Tr1 when a shunted resistor of $400\ \Omega$ is used and the proposed shunted series RL with the same resistance and L is 0.1mH . The figure clearly shows the reduction in both the VFTO magnitude and oscillation in case of the proposed technique. Furthermore, Figure 18 gives an overall comparison between the VFTO when only $400\ \Omega$ shunted resistor is used and both the proposed techniques; shunted series RC ($R=400\ \Omega$ and $C=1\text{pF}$) and shunted series RC ($R=400\ \Omega$ and $L=1\text{mH}$). It is clearly seen that the VFTO due to the proposed shunted series RC is less in magnitude and oscillations.

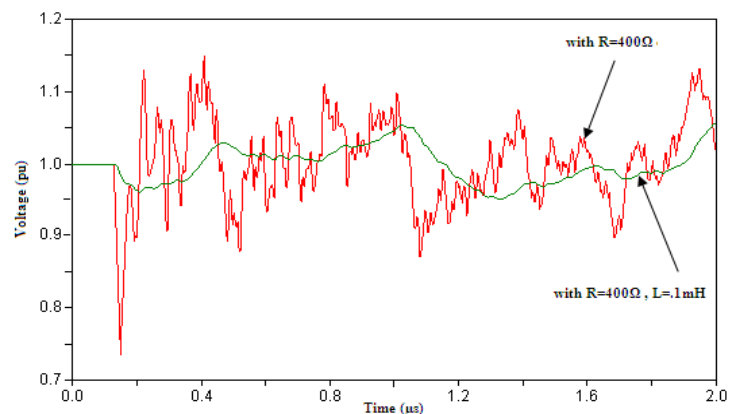


Figure 17. Comparison between the VFTO when either the shunt resistance or the proposed shunted series RL is used

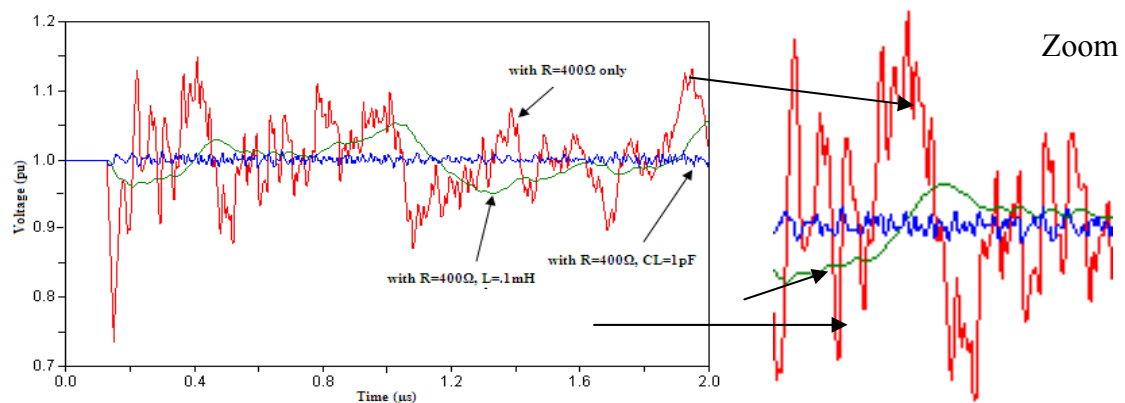


Figure 18. Comparison between the VFTO due to the shunt resistance, the proposed shunted series RC, and the proposed shunted series RL

5.3. Shunted Inductor

VFTOs at transformers are associated with high electric field so utilizing winding of reactor convert electric field into magnetic field and absorb energy of VFTO and reduce it.

Figure (19) shows the VFTO at transformer terminal (Tr1) with and without using a shunt reactor. The inductance of the reactor is used as $1\mu\text{H}$ with the transformer to protect it and also to give an optimum solution. The maximum voltage to ground at transformer, Tr1, Tr2, Tr3, reaches a value of about 1.03, 1.01 and 1.02 pu, respectively, i.e. it reduces by about 49%, 36% and 35%, respectively.

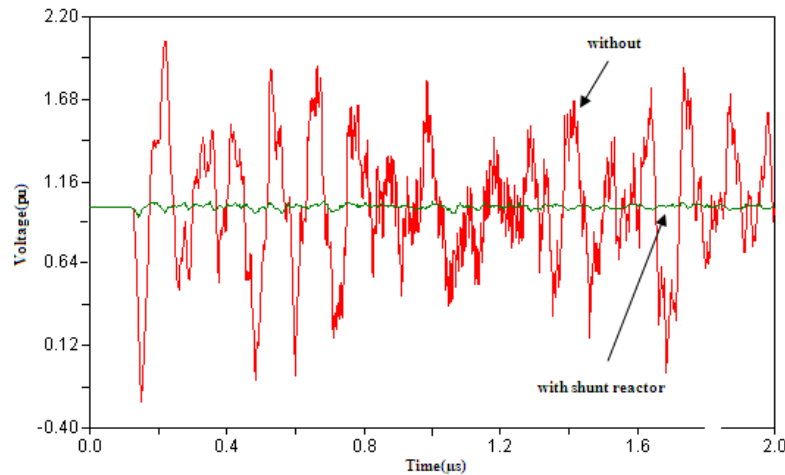


Figure 19. VFTO at Tr1 terminal with and without reactor

6. CONCLUSION

The unexpected problem, VFTO due to switching operation of DS switch in GIS, so the research scopes the study on the worst DS switch operation and study mitigation methods.

The points near switching operation have high amplitude and high oscillation frequency of VFTO as compared the way point.

The main challenges are the reduction in VFTO amplitudes and finally the reduction of the effects of VFTO on the equipment. Also from this study there are two way for mitigation of VFTO in GIS.

Mitigation methods used when substation under operation such as appropriate terminal component as cable, entrance capacitance, R-C filter and shunt reactor. I advise these methods are used in 220kV wadi hoff GIS because low cost implementation as well as minimum changes in the installed GIS (which is currently under operation) are the main advantages of this method.

Because of impossibility of adding capacitance in high voltage systems, the suggestion are the coupling capacitor voltage transformer with capacitance (10nF) is utilized instead of potential transformer or use extra surge arrester with capacitor 10nf or use shunt capacitor with surge arrester or utilize capacitance in underground cable.

Before starting the design of a HV substation, Installing shunt resistor on disconnector can decrease VFTO peak but has not effect on oscillation, so shunt resistor in series with capacitor used to reduce VFTO amplitude and vanish oscillation frequent, also ferrite rings can obviously decrease the amplitude and steepness of VFTO.

REFERENCES

- [1] AJ Martinez. "Statistics Assessment of Very Fast Transient Overvoltages in Gas Insulated Substations". *IEEE Power Engineering Society Summer Meeting*. 2000; 2: 882–883.
- [2] X Dong, S Rosado, Y Liu, NC Wang, EL Line and TY Guo. "Study of Abnormal Electrical Phenomena Effects on GSU Transformers". *IEEE Transactions on Power Delivery*. 2003; 18(3): 835.
- [3] V Vinod Kumar, M Joy Thomas, and MS Naidu. "Influence of Switching Conditions on the VFTO Magnitudes in a GIS". *IEEE Transaction on Power Delivery*. 2001; 16(4).
- [4] M Mohana Rao, M Joy Thomas, and BP Singh. "Electromagnetic Field Emission from Gas-to-Air Bushing in a GIS During Switching Operations". *IEEE Transactions on Electromagnetic Compatibility*. 2007; 49(2).

- [5] L Qingmin and W Minglei. "Simulation Method for the Applications of Ferromagnetic Materials in Suppressing High Frequency Transients within GIS". *IEEE Transactions on Power Delivery*. 2007; 22(3): 1628.
- [6] Mariusz Stosur, Marcin Szewczyk, Wojciech Piasecki, Marek Florkowski and Marek Fulczyk. "GIS Disconnect Switching Operation – VFTO Study". Modern Electric Power Systems. 2010, MEPS'10 - paper 13.4, Wroclaw, Poland.
- [7] JVG Rama Rao, J Amarnath and S Kamakshaiah. "Accurate Modeling of Very Fast Transients Overvoltages in A 245kV GIS and Research on Protection Measures". *IEEE International conference on Electrical Insulation and Dielectric phenomena (CEIDP2010)*, West Lafayette, USA.
- [8] Wang Zhuo, Wang Weiquan and Wang Qiang. "Research of Suppressing VFTO for 500kV GIS Substation Based on EMTP/ATP". *International Conference on E -Business and E -Government (ICEE)*. 6-8 May 2011.
- [9] Wan Yiru, Chen Guang and Zhou Hao. "Study on VFTO in UHV GIS Substation". 4th International Conference on Electric Utility Deregulation and Restructuring and Power Technologies (DRPT), 2011.
- [10] Ahmad Tavakoli, Ahmad Gholami, "Influence of Terminal Components for Suppression of High-Frequency Transients in GIS". *International Power and Energy Conference (IPEC 2010)*, Singapore, 27-29 Oct. 2010.

BIOGRAPHIES OF AUTHORS



Mousa A Abd-Allah was born in Cairo, Egypt, on August 16, 1961. He received the B.Sc. degree in electrical Engineering with honor in 1984 and the M.Sc. degree in High Voltage Engineering in 1988, both from Zagazig university, benha branch, Cairo, Egypt. He received the Ph.D. degree in High Voltage Engineering in 1992 from Cairo university. He is currently a professor with the Electrical Engineering department, Faculty of Engineering at Shoubra, Benha university. His research activity includes Electromagnetic Field Assessment and Mitigation around Electrical Equipments, Gas discharge in gas insulated systems, Electromagnetic Compatibility, Transient Phenomenon in Power Networks.



A Said was born in Cairo, Egypt, on March 9, 1987. He received the B.Sc. degree in electrical engineering with honor degree in 2009 and the M.Sc. degree in High voltage engineering in 2013, both from Faculty of Engineering at Shoubra, Benha University, Cairo, Egypt. On August 2010, he received his work in this faculty as an instructor in the Electrical Engineering Department. Currently he is assist lecture and PHD researcher in high voltage engineering. His research activity includes studying the transient in all components of GIS, factor affecting on VFTO, mitigation method of VFTO.



Ebrahim A Badran was born in Fareskor, Damietta, Egypt, on January 10, 1969. He received the B.Sc. degree in electrical Engineering with honor in 1991 and the M.Sc. degree in Electrical power and machines in 1995, both from Mansoura university, Cairo, Egypt. He received the Ph.D. degree in Electrical power and machines in 2004 from Mansoura university. He is currently a Lecturer with The Electrical Engineering Department, Mansoura University and IEEE member. His research activity includes studying the transient in all component of GIS, factor affecting on VFTO, mitigation method of VFTO. Transformer modeling, ferro resonance, Electrical drives.